Opt Rev (2016) 23:354–359
DOI 10.1007/s10043-015-0171-9

SPECIAL SECTION: REGULAR PAPER

The 5th Asian and Pacific-Rim Symposium on Biophotonics, (APBP'15), Yokohama, Japan

In vivo estimation of optical properties of rat liver using single-reflectance fiber probe during ischemia and reperfusion

Sharmin Akter[1] · Tomoki Tanabe[1] · Satoshi Maejima[2] · Satoko Kawauchi[3] · Shunichi Sato[3] · Akinari Hinoki[2] · Suefumi Aosasa[2] · Junji Yamamoto[2] · Izumi Nishidate[1]

Received: 31 August 2015 / Accepted: 18 December 2015 / Published online: 31 December 2015

Abstract To quantify the changes in optical properties of in vivo rat liver tissue, we applied diffuse reflectance spectroscopy (DRS) system using single-reflectance fiber probe during ischemia and reperfusion evoked by hepatic portal occlusion (hepatic artery, portal vein and bile duct). Changes in the reduced scattering coefficient μ_s', the absorption coefficient μ_a, the tissue oxygen saturation StO_2, and the oxidation of heme aa3 in cytochrome *c* oxidase (C*c*O) $OHaa_3$ of in vivo rat liver ($n = 6$) were evaluated. Heme aa_3 in C*c*O were significantly reduced ($P < 0.05$) during ischemia, which indicates a sign of mitochondrial energy failure induced by oxygen insufficiency of liver tissue. We found that $OHaa_3$ obtained from the proposed method was unchanged immediately after the onset of ischemia and started gradually decreasing at 2 min after the onset of ischemia. Difference in the time course between $OHaa_3$ and the conventional ratio metric analysis with $\mu_a(605)/\mu_a(620)$ reported in literature demonstrates that the proposed method is effective in reduction of optical cross talk between hemoglobin and heme aa_3. Our results suggest that DRS technique is applicable and useful for assessing in vivo tissue viability and hemodynamics in liver intraoperatively.

✉ Izumi Nishidate
inishi@cc.tuat.ac.jp

[1] Graduate School of Bio-Application and Systems Engineering, Tokyo University of Agriculture and Technology, 2-24-16 Naka-cho, Koganei, Tokyo 184-8588, Japan

[2] Department of Surgery, National Defense Medical College, Tokorozawa, Saitama 359-8513, Japan

[3] Division of Biomedical Information Sciences, National Defense Medical College Research Institute, Tokorozawa, Saitama 359-8513, Japan

Keywords Diffuse reflectance spectroscopy · Absorption coefficient · Reduced scattering coefficient · Tissue oxygen saturation · Cytochrome *c* oxidase · Liver ischemia–reperfusion

1 Introduction

Liver ischemia–reperfusion could induce hepatocellular injury such as apoptosis, cell death and necrosis, that usually occur as a consequence of partial hepatic resection surgery, liver transplantation and hemorrhagic shock with fluid resuscitation [1]. Post-transplant complications such as hepatic artery occlusion, portal vein thrombosis, primary non-function, and acute graft rejection cause impairment of liver graft microcirculation and tissue hypoxia with eventual loss of the graft without early intervention [2]. Clamping of hepatic portal during partial liver resection leads to ischemia in the remnant liver, while during reperfusion, additional liver injury is added to the damage already sustained during reperfusion. As liver function depends on tissue oxygen supply, measurement of hepatic tissue oxygenation has been shown to correlate significantly with the microcirculatory liver failure and liver dysfunction induced by ischemia–reperfusion injury [3]. In hepatocytes, about 90 % of the oxygen taken up is consumed by heme aa_3 in C*c*O in mitochondria [4]. Therefore, assessment of the redox state of heme aa_3 in cytochrome *c* oxidase (C*c*O) could be used as a potential indicator of cellular energy level [5] and the severity of hepatic ischemia–reperfusion injury [3].

In general, optical measurements, including in vivo spectroscopy, have been widely used for monitoring tissue hemodynamics in liver tissue [6]. Diffuse reflectance spectroscopy provides a wealth information about tissue

composition, which is minimally invasive or non-invasive to the in vivo biological tissue, and can be fine-tuned for the specific clinical application by changing the source-detector-separation, the fiber geometry, and/or the wavelength range [7]. The spectral shape and magnitude are reflective of the absorption and scattering properties of the tissue. Thus, the wavelength dependent absorption and reduced scattering coefficients of the tissue (μ_a and μ_s', respectively) can be extracted using various theoretical and numerical models. Subsequently, the collected spectral information is further translated into morphologic and physiologic information.

We have investigated a method with a single-reflectance optical fiber probe to evaluate the reduced scattering coefficient spectrum $\mu_s'(\lambda)$, the absorption coefficient spectrum $\mu_a(\lambda)$, the tissue oxygen saturation StO_2, and the reduction of heme aa_3 in C*c*O of in vivo liver tissue [8]. The method calculated StO_2 based on the regression coefficients obtained from the multiple regression analysis using the estimated absorption coefficient spectrum $\mu_a(\lambda)$ as a response variable and the extinction coefficient spectra of oxygenated hemoglobin and deoxygenated hemoglobin as predictor variables. On the other hand, the ratio of μ_a at 605 nm and that of at 620 nm was used to evaluate the oxidation of heme aa_3 in C*c*O. Basically, optical evaluation of a chromophore in vivo can suffer from optical cross talk from absorption signals by the other chromophores. Therefore, the measurements of StO_2 derived from the method could be varied with the changes in the concentrations of oxidized heme aa_3 and reduced heme aa_3. Similarly, the value of $\mu_a(605)/\mu_a(620)$ could be fluctuated by the changes in the concentrations of oxygenated hemoglobin and deoxygenated hemoglobin. To perform more accurate evaluations of the tissue oxygen saturation and the redox state of heme aa_3, the above four chromophores should be taken into account in the analysis of the estimated $\mu_a(\lambda)$.

In the present study, we newly propose a method of the multiple regression analysis for the estimated $\mu_a(\lambda)$ with the extinction coefficient spectra of oxygenated hemoglobin, deoxygenated hemoglobin, oxidized heme aa_3, and reduced heme aa_3. To confirm the validity of the method for evaluating the tissue oxygen saturation and the oxidation of heme aa_3 in C*c*O of liver tissue, we performed in vivo experiments using exposed rat liver before and during ischemia–reperfusion induced by the occlusion of the hepatic portal.

2 Principle

2.1 Reflectance fiber probe system

The reflectance fiber probe system with the two source-detection geometries developed by Nishidate et al. [10] was used in the present study. The system consists of a light source, bifurcated fiber, a reflectance fiber probe, and two spectrometers under the control of a personal computer. The bifurcated fiber has two optical fibers of the same diameter of 400 μm placed side by side in the common end. The reflectance fiber probe has a 600-μm-diameter fiber in the center surrounded by six 600-μm-diameter fibers. One end of the center fiber of the reflectance fiber probe is connected to the common end of the bifurcated fiber through a fiber connector. A halogen lamp light source (HL-2000, Ocean Optics Inc., Dunedin, FL, USA), which covers the visible to NIR wavelength range, is used to illuminate the liver tissue via one lead of the bifurcated fiber and the central fiber of the reflectance fiber probe. Diffusely reflected light from the sample is detected by both the central fiber and the six surrounding fibers. The center-to-center distances between the central fiber and the surrounding fibers are 700 μm. The light detected by the central fiber is delivered to a multichannel spectrometer (USB4000, Ocean Optics Inc.) via another lead of the bifurcated fiber, whereas that detected by the six surrounding fibers is delivered to the other multichannel spectrometer (USB4000, Ocean Optics Inc.). A solution of Intralipid 10 % [9] was used to calibrate the spectral responses of both spectrometers as a reference material. Diffuse reflectance spectra $R_c(\lambda)$ and $R_s(\lambda)$ ranging from 500 to 800 nm were calculated from the spectral intensities of light detected by the central fiber and the six surrounding fibers, respectively, based on the spectra of reflected light intensity from the reference material.

2.2 Determination of empirical formulas for estimating μ_s' and μ_a

Figure 1a shows the flowchart of the process for estimating μ_s' and μ_a from the measurements of R_c and R_s. We consider the following empirical formula based on the results of the Monte Carlo simulation:

$$\begin{bmatrix} \mu_s' \\ \mu_a \end{bmatrix} = \begin{bmatrix} \alpha_c & \alpha_s \\ \beta_c & \beta_s \end{bmatrix} \begin{bmatrix} A_c \\ A_s \end{bmatrix} \tag{1}$$

where $A_c = -\log_{10} R_c$ and $A_s = -\log_{10} R_s$ are the apparent absorbances for the recording by the center fiber and the surrounding fibers, respectively. To improve the accuracy of Eq. (1), we used the higher-order terms of A_c and A_s in Eq. (1) as follows:

$$\begin{bmatrix} \mu_s' \\ \mu_a \end{bmatrix} = \begin{bmatrix} \alpha_0 & \alpha_1 & \alpha_2 & \alpha_3 & \alpha_4 & \alpha_5 \\ \beta_0 & \beta_1 & \beta_2 & \beta_3 & \beta_4 & \beta_5 \end{bmatrix} \begin{bmatrix} 1 & A_c^2 & A_s^2 & A_c A_s & A_c & A_s \end{bmatrix}^t \tag{2}$$

where $[]^t$ represents the transposition of a vector. Coefficients α_i and β_i ($i = 0, 1, 2, 3, 4, 5$) in Eq. (2) can be

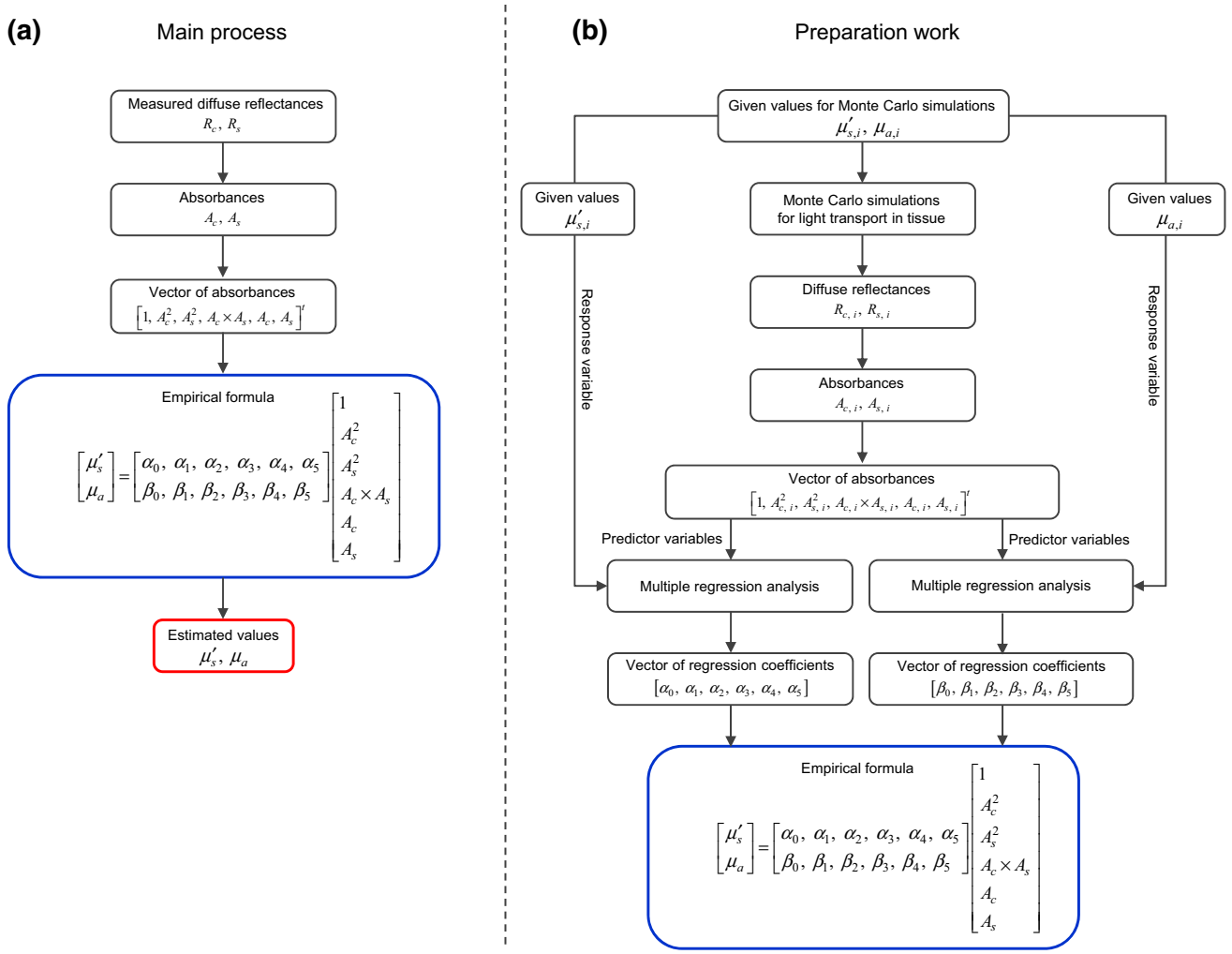

Fig. 1 Flowchart of the process for estimating $\mu_s'$and μ_a from the measured diffuse reflectance R_c and R_s. **a** Main process for μ_s' and μ_a and **b** preparation work for determining empirical formulae

determined statistically by multiple regression analysis of the results of the Monte Carlo simulations as shown in Fig. 1b. The details of the Monte Carlo simulation model were published previously [8, 10]. In the Monte Carlo simulations, R_c and R_s were calculated for the ranges of $\mu_a = 0.1$–$80\ \mathrm{cm}^{-1}$ and $\mu_s' = 5.0$–$80\ \mathrm{cm}^{-1}$. The values of $\mu_s'(\lambda)$ and $\mu_a(\lambda)$ can be estimated by applying Eq. (2) to each wavelength point of $A_c(\lambda)$ and $A_s(\lambda)$.

2.3 Evaluation of tissue oxygen saturation and redox state of heme aa_3 in cytochrome *c* oxidase from $\mu_a(\lambda)$

The absorption coefficient spectrum is given by the sum of absorption due to oxygenated hemoglobin, deoxygenated hemoglobin, oxidized heme aa_3, and reduced heme aa_3. Using the absorption coefficient spectrum $\mu_a(\lambda)$ as a response variable and the extinction coefficient spectra of $\varepsilon_{HbO}(\lambda)$ [11], $\varepsilon_{HbR}(\lambda)$ [11], $\varepsilon_{HmO}(\lambda)$ [12] and $\varepsilon_{HmR}(\lambda)$ [12] as predictor variables, the multiple regression model can be express as follows:

$$\mu_a(\lambda_k) = a_{HbO} \times \varepsilon_{HbO}(\lambda_k) + a_{HbR} \times \varepsilon_{HbR}(\lambda_k) + a_{HmO} \times \varepsilon_{HmO}(\lambda_k) + a_{HmR} \times \varepsilon_{HmR}(\lambda_k) + a_0 + e(\lambda_k) \quad (3)$$

where a_{HbO}, a_{HbR}, a_{HmO}, a_{HmR}, and a_0 are the regression coefficients, $e(\lambda_k)$ is an error component, and λ_k indicates discrete values in the wavelength range treated in the analysis. Subscripts HbO, HbR, HmO, and HmR denote oxygenated hemoglobin, deoxygenated hemoglobin, oxidized heme aa_3, and reduced heme aa_3, respectively. By executing the multiple regression analysis for one sample of the absorption coefficient spectrum consisting of p discrete wavelengths, one set of the three regression coefficients is obtained. In this case, the regression coefficient a_0 is a constant component or an intercept and expressed as follows:

$$a_0 = \bar{\mu}_a - \bar{\varepsilon}_{HbO} a_{HbO} - \bar{\varepsilon}_{HbR} a_{HbR} - \bar{\varepsilon}_{HmO} a_{HmO} - \bar{\varepsilon}_{HmR} a_{HmR} \quad (4)$$

where $\bar{\mu}_a$, $\bar{\varepsilon}_{HbO}$, $\bar{\varepsilon}_{HbR}$, $\bar{\varepsilon}_{HmO}$, and $\bar{\varepsilon}_{HmR}$ are the averages of $\mu_a(\lambda_k)$, $\varepsilon_{HbO}(\lambda_k)$, $\varepsilon_{HbR}(\lambda_k)$, $\varepsilon_{HmO}(\lambda_k)$, and $\varepsilon_{HmR}(\lambda_k)$ over the wavelength range, or $k = 1$–p. In the present study, we used the spectrum of absorption coefficient in the range from 520 to 600 nm at intervals of 10 nm for the multiple regression analysis to evaluate both the oxidation of heme aa_3 in C*c*O and the tissue oxygen saturation because the spectral features of oxygenated hemoglobin, deoxygenated hemoglobin, oxidized heme aa_3, and reduced heme aa_3 notably appear in this wavelength range. The regression coefficients a_{HbO}, a_{HbR}, a_{HmO}, and a_{HmR} describe the degree of contributions of $\varepsilon_{HbO}(\lambda)$, $\varepsilon_{HbR}(\lambda)$, $\varepsilon_{HmO}(\lambda)$, and $\varepsilon_{HmR}(\lambda)$, respectively, to the absorption coefficient spectrum $\mu_a(\lambda)$ and, consequently, are closely related to the concentrations of oxygenated hemoglobin, deoxygenated hemoglobin, oxidized heme aa_3, and reduced heme aa_3, respectively. The oxygen saturation of hemoglobin, StO_2, is defined as the ratio of the oxygenated hemoglobin concentration in the total hemoglobin concentration. In this study, the oxygen saturation is estimated from the regression coefficients a_{HbO} and a_{HbR} as follows:

$$StO_2 = \frac{a_{HbO}}{a_{HbO} + a_{HbR}} \quad (5)$$

Similarly, we also used the estimated absorption coefficient spectrum $\mu_a(\lambda)$ to evaluate the oxidation of heme aa_3 in C*c*O. In this study, we newly propose the method to evaluate the oxidation of heme aa_3 ($OHaa_3$) using the regression coefficients a_{HmO} and a_{HmR} as follows:

$$OHaa_3 = \frac{a_{HmO}}{a_{HmO} + a_{HmR}} \quad (6)$$

Thus, the current analysis on the oxidation of heme aa_3 is different from the ratio metric analysis proposed previously [8] in terms of the use of the regression coefficients a_{HmO} and a_{HmR}. The current analysis uses the regression coefficients a_{HmO} and a_{HmR} derived from the multiple regression analysis to evaluate the redox state of heme aa_3 in C*c*O whereas the previous analysis [8] relies on the ratio of μ_a (605) and μ_a (620). On the other hand, there are two similarities between the current analysis and previous one [8]. One is the process for estimating μ_s' and μ_a from the diffuse reflectance R_c and R_s measured by the reflectance fiber probe system developed by Nishidate et al. [10]. The other is the use of wavelength-dependences of absorption by both reduced heme aa_3 and oxidized heme aa_3 to evaluate the redox state of heme aa_3 in C*c*O.

3 Experiments

Six male Wister rats weighing from 132 to 458 g were maintained at 27 °C with a 12/12-h dark/light cycle and allowed food and water ad libitum. Experiments performed in the present study were approved by the Animal Research Committee of Tokyo University of Agriculture and Technology. Rats were anesthetized by intraperitoneal injection of a mixture of α-chloralose (50 mg/kg) and urethane (600 mg/kg). After laparotomy was performed by a transversal incision, the ligaments around the liver lobes were dissected to mobilize the left lobe. At the same time, the hepato-duodenal ligament was taped in preparation for further clamping. Hepatic ischemia was induced by clamping the hepatic portal (the hepatic artery, the portal vein, and the bile duct) for 30 min, followed by declamping. Anoxic condition was induced by nitrogen breathing at 60 min after the onset of reperfusion to sacrifice the rats. The caudate lobe of the liver was kept as a passage for the portal blood. The reflectance fiber probe was placed on the surface of the liver lobe. Measurements of $R_c(\lambda)$ and $R_s(\lambda)$ were obtained simultaneously in the wavelength range of from 500 to 800 nm at 30 s intervals for 100 min: oxygen breathing for 5 min, normal air breathing for 5 min, ischemia for 30 min, and reperfusion for 60 min. Estimation of $\mu_s'(\lambda)$ and $\mu_a(\lambda)$ was performed based on the process described above. Data are presented as mean ± SD. An unpaired *t* test was performed to compare the average values over the samples between the normal (Air breathing) and the other periods (oxygen breathing, ischemia, and reperfusion) and $P < 0.05$ was considered significant.

4 Results and discussion

Figure 2a shows the typical time courses of $OHaa_3$ during the period of pre-ischemia (oxygen breathing and air breathing), ischemia, and reperfusion. Enlarged view of the part enclosed by a dashed blue square in Fig. 2a is also shown in Fig. 2b. The average values of $OHaa_3$ averaged over six samples are averaged over each period and are summarized in Fig. 3. In the previous study [8], the tissue oxygen saturation StO_2 was rapidly dropped immediately after the onset of ischemia and was decreased to around 0 % at 1 min after the onset of ischemia. In contrast, $OHaa_3$ obtained from the proposed method was unchanged immediately after the onset of ischemia as shown in Fig. 2b. The value of $OHaa_3$ was significantly decreased at 2 min after the onset of ischemia, representing a reduction in heme aa_3, which is a sign of mitochondrial energy failure. After 40 min of reperfusion, the value of $OHaa_3$ reverted to the pre-ischemic level. It should be noted that

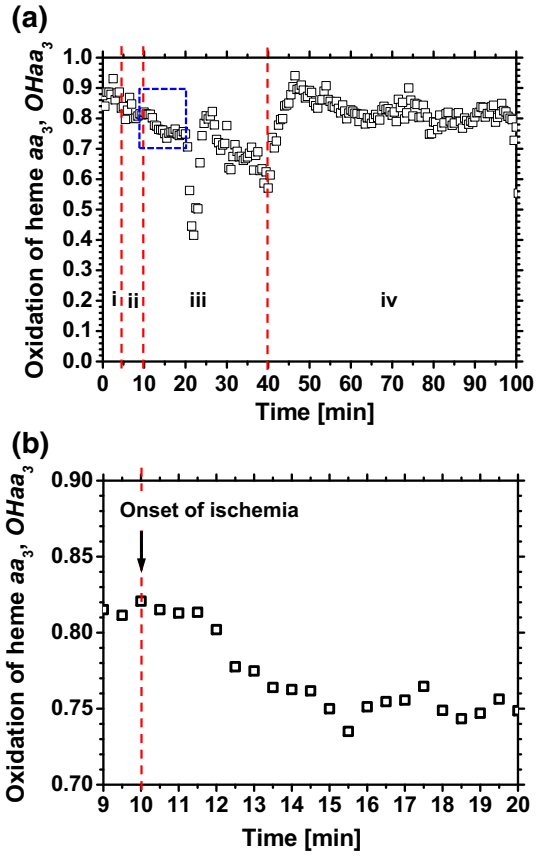

Fig. 2 **a** Typical time course of the oxidation of heme aa_3 in cytochrome *c* oxidase $OHaa_3$ during ischemia-reperfusion experiments. Roman numerals, *i*, *ii*, *iii*, and *iv* represent oxygen breathing, air breathing, ischemia under air breathing, and reperfusion under air breathing, respectively. **b** Enlarged view of the part enclosed by a *dashed blue square* in (**a**)

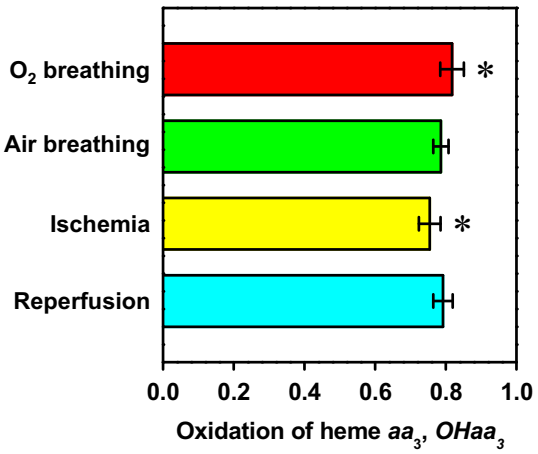

Fig. 3 Average values of the oxidation of heme aa_3 in cytochrome *c* oxidase $OHaa_3$ over the six samples averaged over each period

$OHaa_3$ started gradually decreasing at 2 min after the onset of ischemia and was not synchronized with the tissue oxygen saturation. This may be due to the difference in oxygen affinity between the heme aa_3 in C*c*O and hemoglobin and corresponds to the relationship between the relative oxidation state of cytochrome *c* oxidase with respect to the relative oxygenation state of hemoglobin [13]. Hoshi et al. [13] have shown that the redox state of cytochrome *c* oxidase was remained unchanged and independent of the oxygen state of hemoglobin until the relative change in oxygen state of hemoglobin decreased to approximately 40 %. In the range of lower than this level of the relative change in oxygenation state of hemoglobin, the cytochrome *c* oxidase was decreased almost linearly with the decrease in the oxygen state of hemoglobin. In our previous report [8], immediately after the onset of ischemia, the index of reduction of heme aa_3 defined by the ratio of $\mu_a(605)/\mu_a(620)$ was rapidly increased and was synchronized with the tissue oxygen saturation StO_2. Difference in the time course between $OHaa_3$ during ischemia shown in Fig. 2 and $\mu_a(605)/\mu_a(620)$ reported in the previous study [8] demonstrates that the proposed method with $OHaa_3$ is effective in reduction of optical cross talk between hemoglobin and heme aa_3. The average value of $OHaa_3$ was 0.82 ± 0.03 during oxygen breathing, 0.79 ± 0.02 during normal air breathing before ischemia, 0.75 ± 0.03 during ischemia, and 0.79 ± 0.03 during reperfusion. The results showed that the current DRS system could effectively monitor the reduction of heme aa_3 in C*c*O resulting from the hepatic occlusion, which reflects the ischemia-induced microcirculatory dysfunction in the liver [14, 15]. Liver transplantation would be one useful clinical application of this technology because an adequate blood supply and tissue oxygenation of the graft is essential to its initial functioning [16, 17]. The results of $OHaa_3$ indicate that the method applied in the present study is reliable and has potential application in the intraoperative assessment of graft tissue viability.

5 Conclusions

We investigated a method for evaluating the reduced scattering coefficient, the absorption coefficient, the tissue oxygen saturation, and the oxidation of heme aa_3 in cytochrome *c* oxidase of in vivo liver tissue using a single-reflectance fiber probe system. Difference in the time course between $OHaa_3$ and the conventional ratio metric analysis with $\mu_a(605)/\mu_a(620)$ demonstrates that the proposed method could effectively reduce optical cross talk between hemoglobin and heme aa_3. The results of the present study indicate the potential application of the current DRS system in evaluating the oxygen levels and pathophysiological conditions of in vivo liver tissue. Since the proposed method can be used to simultaneously evaluate changes in hemodynamics, mitochondrial energy

level, and tissue morphology, this method will be effective for studying pathophysiological conditions of in vivo liver tissue. We intend to further extend the proposed method to monitor tissue viability resulting from liver transplantation.

References

1. Cursio, R., Colosetti, P., Saint-Paul, M.C., Pagnotta, S., Gounon, P., Iannelli, A., Auberger, P., Gugenheim, J.: Induction of different types of cell death after normothermic liver ischemia-reperfusion. Transplant. Proc. **42**(10), 3977–3980 (2010)
2. Kiuchi, T., Schlitt, H.J., Oldhafer, K.J., Nashan, B., Tanaka, A., Wonigeit, K., Ringe, B., Tanaka, K., Yamaoka, Y., Pichlmayr, R.: Early acute rejection after hepatic graft reperfusion: association with ischemic injury with good function, oxygenation heterogeneity, and leukocyte adhesion without aggregation. Transplant. Proc. **29**(1–2), 364–365 (1997)
3. El-Desoky, A.E., Delpy, D.T., Davidson, B.R., Seifalian, A.M.: Assessment of hepatic ischaemia reperfusion injury by measuring intracellular tissue oxygenation using near infrared spectroscopy. Liver **21**(1), 37–44 (2001)
4. de Groot, H., Noll, T.: Halothane-induced lipid peroxidation and glucose-6-phosphatase inactivation in microsomes under hypoxic conditions. Anesthesiology **62**(1), 44–48 (1985)
5. Chandel, N.S., Budinger, G.R., Choe, S.H., Schumacker, P.T.: Cellular respiration during hypoxia. Role of cytochrome oxidase as the oxygen sensor in hepatocytes. J. Biol. Chem. **272**(30), 18808–18816 (1997)
6. Sato, N., Hayashi, N., Kawano, S., Kamada, T., Abe, H.: Hepatic hemodynamics in patients with chronic hepatitis or cirrhosis as assessed by organ-reflectance spectrophotometry. Gastroenterology **84**(3), 611–616 (1983)
7. Bydlon, T.M., Nachabé, R., Ramanujam, N., Sterenborg, H.J., Hendriks, B.H.: Chromophore based analyses of steadystate diffuse reflectance spectroscopy: current status and perspectives-for clinical adoption. J. Biophotonics **8**(1–2), 9–24 (2015)
8. Akter, S., Maejima, S., Kawauchi, S., Sato, S., Hinoki, A., Aosasa, S., Yamamoto, J., Nishidate, I.: Evaluation of light scattering and absorption properties of in vivo rat liver using a single-reflectance fiber probe during preischemia, ischemia-reperfusion, and postmortem. J. Biomed. Opt. **20**(7), 076010 (2015)
9. van Staveren, H.J., Moes, C.J., van Marie, J., Prahl, S.A., Gamert, M.J.: Light scattering in Intralipid-10 % in the wavelength range of 400–1100 nm. Appl. Opt. **30**(31), 4507–4514 (1991)
10. Nishidate, I., Mizushima, C., Yoshida, K., Kawauchi, S., Sato, S., Sato, M.: In vivo estimation of light scattering and absorption properties of rat brain using a single-reflectance fiber probe during cortical spreading depression. J. Biomed. Opt. **20**(2), 027003 (2015)
11. Prahl, S.A.: Tabulated molar extinction coefficient for hemoglobin in water. http://omlc.ogi.edu/spectra/hemoglobin/summary.html (1999)
12. Cytochrome Spectra. http://www.ucl.ac.uk/medphys/research/borl/intro/spectra (2005)
13. Hoshi, Y., Hazeki, O., Kakihana, Y., Tamura, M.: Redox behavior of cytochrome oxidase in the rat brain measured by near-infrared spectroscopy. J. Appl. Physiol. **83**(6), 1842–1848 (1997)
14. Li, C.H., Wang, H.D., Hu, J.J., Ge, X.L., Pan, K., Zhang, A.Q., Dong, J.H.: The monitoring of microvascular liver blood flow changes during ischemia and reperfusion using laser speckle contrast imaging. Microvasc. Res. **94**, 28–35 (2014)
15. Vollmar, B., Glasz, J., Post, S., Menger, M.D.: Role of microcirculatory derangements in manifestation of portal triad cross-clamping-induced hepatic reperfusion injury. J. Surg. Res. **60**(1), 49–54 (1996)
16. Goldstein, R.M., Secrest, C.L., Klintmalm, G.B., Husberg, B.S.: Problematic vascular reconstruction in liver transplantation. Part I. Arterial. Surgery **107**(5), 540–543 (1990)
17. Payen, D.M., Fratacci, M.D., Dupuy, P., Gatecel, C., Vigouroux, C., Ozier, Y., Houssin, D., Chapuis, Y.: Portal and hepatic arterial blood flow measurement of human transplanted livers by implanted Doppler probes: interest for early complications and nutrition. Surgery **107**(4), 540–543 (1990)